Preprint Version - https://doi.org/10.4031/MTSJ.54.4.6
Published in *Marine Technology Society Journal*, Vol. 54, No. 4, pp. 40-58, 2020.

# Maneuvering Ability based Weighted Potential Field Framework for Multi-USV Navigation, Guidance and Control

Tamzidul Mina[1,2], Yogang Singh[1,3], and Byung-Cheol Min[1]

[1]SMART Lab, Department of Computer and Information Technology, Purdue University, IN 47907, USA
[2]School of Mechanical Engineering, Purdue University, IN 47907, USA
[3]Department of Mechanical Engineering, KU Leuven, 3000, Belgium

**Abstract**
Numerous types of Unmanned Surface Vehicles (USVs) are currently available for different applications with a wide spectrum of maneuvering capabilities. We present a generalized multi-USV navigation, guidance and control framework adaptable to specific USV maneuvering response capabilities for dynamic obstacle avoidance. The proposed method integrates offline optimal path planning with a safety distance constrained A* algorithm, and an online Extended Adaptively Weighted (EAW) artificial potential field based path following approach with dynamic collision avoidance, based on USV maneuvering response times. The framework adaptively weighs inter-USV interaction, waypoint following, and collision avoidance based on USV maneuvering capabilities. The EAW system allows USVs with fast maneuvering abilities to react late and slow USVs to react sooner to oncoming moving obstacles gradually, with a carefully designed series of repulsive potential with diminishing weighting along the predicted path of detected moving obstacles, such that a smooth path is followed by the USV group with reduced cross-track error and reduced maneuvering effort. We emphasize the importance of such requirements in constrained and busy maritime environments such as narrow channels in busy harbors. Simulation results validate the proposed EAW artificial potential field framework for different sized multi-USV teams showing reduced cross-track error and maneuvering effort compared to the unweighted or traditional approach, for both slow and fast maneuvering multi-USV teams.

*Keywords*—multi-vehicle systems, unmanned surface vehicles, weighted potential function, navigation, guidance and control.

## 1. Introduction

This paper is an extended version of the previous work presented in Mina et al., 2019.

Autonomous multi-Unmanned Surface Vehicle (USV) systems have been a popular area of research in marine robotics over the past decade. USVs operating in the maritime environment are employed in various applications such as bathymetric surveys, water monitoring, and data acquisition (Kimball et al., 2014; Fraga et al., 2014; Girdhar et al., 2011; Moulton et al., 2018), with numerous multi-USV applications including aquatic sensing, sampling, oil and pollution cleanup (Dolan et al.,2009; Abidin et al., 2010; Protei, 2011). The proficiencies required for USVs moving as a fleet or as a single entity to be considered autonomous can be grouped into three fields: navigation, guidance and control (NGC) (Stenersen, 2015). The area of navigation in USVs deals with approaches of path planning and obstacle avoidance (Singh et al., 2018; Karapetyan et al., 2019; Xie et al., 2019) while the area of guidance and control in USVs deal with approaches

of path following, collision avoidance and cooperative behaviors (Moulton et al., 2019; Manjanna et al., 2018; Karapetyan et al., 2019; Breivik and Fossen, 2004; Zhao et al., 2016). USV applications requiring navigating narrow waterways such as rivers, port or harbor areas (Mancini et al., 2015; Fraga et al., 2014; Dunbabin et al., 2017) require special care in designing NGC systems where dynamic obstacle avoidance is especially challenging while maintaining small cross-track errors from their prescribed paths.

USVs are available in different sizes, shapes, speed constraints and with different maneuvering capabilities. Development of a generic NGC system for USVs is therefore a significantly challenging task. USVs generally used by the military on surveillance and patrolling applications have high speed capabilities (See, 2017), while USVs used for surveys, measurement or water monitoring tasks operate at slower speeds (Motwani, 2012; Thirunavukkarasu et al., 2017). USVs with varying shapes include the Catamaran type Springer (Naeem et al., 2006), MIT's AutoCat (Manley et al., 2000) and Charlie (Caccia et al., 2006); kayak type USVs developed at MIT (Goudey et. Al, 1998) and *SCOUT* (Curcio et al., 2005) and other low cost small USVs developed specific to different applications (Thirunavukkarasu et al., 2017; Jo et al., 2019). Relevant to heterogenous multi-USV control, CARACaS (Control Architecture for Robotic Agent Command and Sensing) was developed at the NASA Jet Propulsion Laboratory as an autonomy architecture for heterogenous multi-agent systems and provided foundational software infrastructure, core executive functions, and several default robotic technology modules (Wolf et al., 2017). Although a lot of multi-USV path planning and obstacle avoidance research has been proposed in literature, very few has addressed applicability concerns of their proposed method on the wide variety of USVs currently available. Previous research on the topic relevant to our current work is presented below.

The advancements in electronic navigation equipment and sensor technology have led to the development of several path planning and obstacle avoidance approaches for USVs (Larson et al., 2006; Savvaris et al., 2014; Campbell et al., 2014). Several new control approaches have been adopted from the area of mobile robotics and extended to improve the autonomy of USVs as well (Caccia et al., 2008; Sharma et al., 2014; Cui et al., 2017). Most of these studies have been focused on a single USV to improve its overall efficiency in a maritime environment. With the increased requirement of high endurance, better temporospatial data and reduced cost in maritime missions, studies on multi-USV frameworks have gained a lot of momentum in the last decade (Kobilarov, 2012; Liu and Bucknall, 2015; Liu and Bucknall, 2018).

The current study associates with two important areas of research on multi-USV systems: self-organization including formation control; and collision avoidance including path planning and path following in marine environments. Formation control methods have been proposed as behavior-based interactions (Balch et al., 1998; Cao et al., 2003; Arrichiello et al., 2006), leader-follower approaches (Peng et al., 2015), virtual structure (Do, 2012) and artificial potential functions (Huang et al., 2014). An overview of the recent research work on the topic of formation control in USVs can be found summarized in Chen and Wang, 2015; Guanghua et al., 2013 and Oh, 2017. Recent works on path planning and real-time obstacle avoidance using Convention on the International Regulations for Preventing Collisions (COLREGS) without relying on LiDAR or other sensors have been proposed in Beser et al., 2018. Wang et al., 2018 proposed a hybrid approach combining A* algorithm path planning with Dynamic Window for obstacle detection

and avoidance in the maritime environment. Several other methods such as Virtual Target (Bibuli et al., 2018), Bee Colony Dynamics (Oh et al., 2017) and Fast Marching (Liu and Bucknall, 2015) have also been adopted for multi-USV organization and collision avoidance in recent years.

Artificial potential based approaches have been a popular choice for multi-agent self-organization, path following and obstacle avoidance (Manzini, 2017). An improved artificial potential field method has been proposed specifically for USV obstacle avoidance (Xie et al., 2014). An application specific research work was also presented on cooperative searching applications using multi-USV systems (Lin and Liu, 2018). USV navigation method using path planning was proposed with A* algorithm and collision probability distribution modeled by artificial potential fields in Chao et al., 2017; other notable works on collision avoidance based on probabilistic models include Lu et al., 2016.

Most of the path following and obstacle avoidance methods proposed in literature are built on assumptions of specific capabilities of the modeled USVs, and fall short in generalizing their methods to the diverse shapes, weights, sizes, propulsion methods of USVs resulting in different maneuvering capabilities. In our previous work, we presented a novel framework of constrained A* algorithm based offline path planning, and USV maneuvering response time based weighting model that adaptively weighs inter-USV, waypoint following and obstacle repulsion potential field terms for improved performance in path following in terms of reduced cross-track error (Mina et al., 2019). However, the system was only validated with simulations with the assumptions that moving obstacles followed straightforward paths. Therefore, in this paper, in addition to the offline path planning and adaptively weighted inter-USV and waypoint following potential field terms, we propose an Extended Adaptive Weighting (EAW) model based on USV maneuvering response time capabilities, that configures USV and erratically behaving detected moving obstacle repulsion within a limited field-of-view (FOV) as a diminishing series of terms along its predicted path; the complete artificial potential field framework allows improved path following performance for guidance and control in terms of reduced cross-track error and required maneuvering effort for dynamic obstacle avoidance compared to the unweighted (traditional) model.

## 2. Preliminaries and Problem Statement

We consider a fully connected leader-follower group of $n$ USVs on a planar surface $\mathcal{W}$, each denoted as $R_i$, for $i \in I_R = \{1,2,..,n\}$ with position and orientation defined as $r_i = [x_i, y_i]$ and $\theta_i$. Dynamics of each USV is modeled as a unicycle model,

$$\begin{aligned} \dot{x}_i &= v_i \cos\theta_i & \dot{v}_i &= a_i \\ \dot{y}_i &= v_i \sin\theta_i & \dot{\theta}_i &= \omega_i \end{aligned} \tag{1}$$

where $v_i$ and $\dot{\theta}_i$ the linear and angular velocity of $R_i$. The control inputs of $R_i$ are defined as $[u_i, w_i]$, where $u_i = a_i$ and $w_i = \omega_i$. Referring to previous works on radar and LiDAR based obstacle detection for USVs (Almeida, 2009; Halterman, 2010), we assume that all USVs have a circular field of view (FOV) of radius $d$ centered at $(x_i, y_i)$ for simplicity, within which it is able to detect moving and static obstacles. The group leader is denoted as $R_h$, where $h \in I_R$.

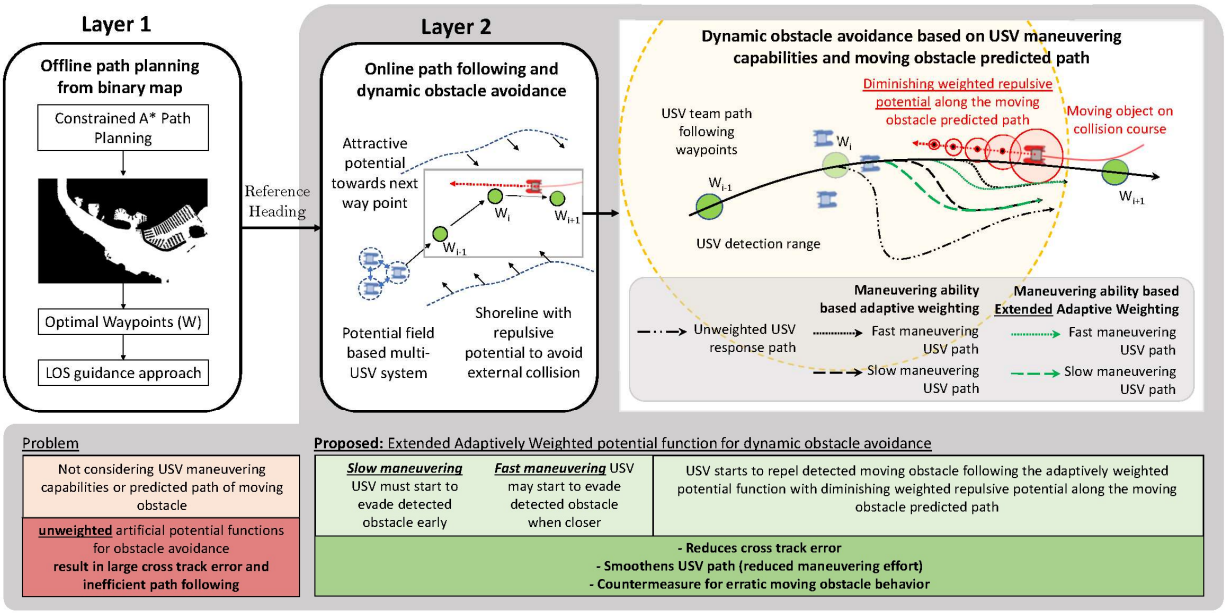


Figure 1: Conceptual illustration of the double layered extended adaptively weighted potential field framework for multi-USV navigation, guidance and control based on USV maneuvering capabilities to reduce cross-track error and maneuvering effort. Layer 1 generates a path from a given map and layer 2 implements path following with extended adaptively weighted collision avoidance and inter-USV dynamics.

Given the wide variety of USVs currently available in the field, we consider a generalized *maneuvering response time unit* for $R_i$ as $t_r$ dependent on its size, weight, maximum speed, braking and various other factors for dynamic obstacle avoidance. For simplicity, we model the effects of $t_r$ on a USV in this paper by limiting the maximum translational acceleration and the maximum turning rate of the USV denoted as $a_{max}$ and $\omega_{max}$. We denote moving obstacles in $\mathcal{W}$ as $M_i$, for $i \in I_M = \{1,2,..,P_m\}$ with position $m_i$ and stationary obstacles on the plane as $O_i$, for $i \in I_O = \{1,2,..,P_o\}$ with position $o_i$. The maneuvering ability of detected moving obstacles are assumed to be unknown.

The objective is for all $n$ USVs to safely navigate through a given environment following an optimally generated path, aggregating and avoiding moving obstacles using our proposed extended adaptively weighted potential function framework based on USV maneuvering response time $t_r$ for reduced cross track error and maneuvering effort.

## 3. Proposed Solution

The proposed generalized multi-USV navigation, guidance and control framework with dynamic obstacle avoidance in a constrained environment consists of two layers. On the top level of the hierarchy (layer 1), an offline robust path planner based on the constrained A* approach (Singh et al., 2018) is adopted to generate optimal way points, which are used to generate reference heading for guidance using the line-of-sight (LOS) method. The reference heading is fed into the lower hierarchy (layer 2) of online path following based on a proposed EAW artificial potential function framework for USV interaction, a diminishing series based dynamic obstacle avoidance along the predicted path of detected moving obstacles, and waypoint following. The novelty of the

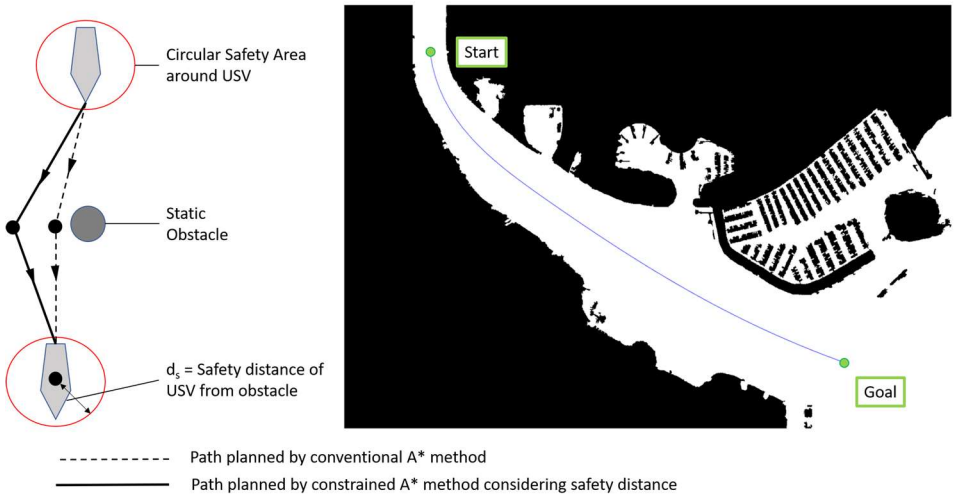


Figure 2: Schematic of the path generated from the path planner in Layer 1 (left) in (Singh et al., 2018) and the generated path along a narrow channel in the Port of Los Angeles harbor area (right).

study lies in this level where the potential function terms of inter-USV interaction, way point attraction and moving obstacle avoidance are adaptively weighted based on USV maneuvering response times to reduce cross track error and maneuvering effort during dynamic collision avoidance, while navigating in an environment with moving vessels. Figure 1 shows the schematic of the double layered EAW framework for the multi-USV system.

*3.1 Layer 1: Constrained A* Path Planning*

In this study, a computationally efficient constrained A* approach has been adopted towards offline path planning for the multi-USV group to form layer 1 of the proposed multi-USV framework (Singh et al., 2018). In this layer, a safety distance constrained A* approach, where the USV is enclosed by a certain safety distance $d_s$ is applied to determine the way points for navigation. The adopted A* approach in this study considers a circle enclosing the USV as safety distance, as shown in Figure 2 (left). We denote the way points generated by the proposed approach as $w_i$, for $i \in I_W = \{1,2,..,P_w\}$ in order.

*3.2 Layer 2: Online Path Following with Dynamic Obstacle Avoidance*

*1) Adaptive weighting model based on USV maneuverability response times*

An exponential based adaptive weighting model is proposed to accommodate USVs with different maneuverability response times $t_r$ in relation to distance to the detected moving object $d_m$,

$$w_s = e^{-\frac{K_w d_m}{t_r}} \tag{2}$$

where $K_w$ is a positive scaling constant for $w_s \in (0,1)$.

Figure 3 illustrates the resulting relationship of $w_s$ with $0 < d_m(m) \leq 100$, $0 < t_r(s) \leq 10$ and $K_w = 0.2$. For large $t_r$, a higher weighting $w_s$ is obtained over decreasing $d_m$. In contrast, for low $t_r$ cases, weighting $w_s$ remains relatively low at higher $d_m$ but quickly increases at lower $d_m$.

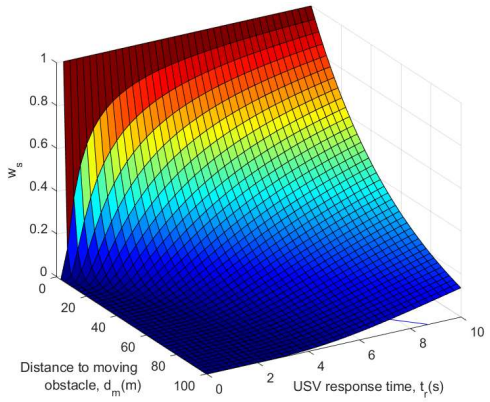


Figure 3: Adaptive weighting model based on moving obstacle distance $d_m$ and USV maneuvering response time $t_r$, for $K_w = 0.2$.

We justify our choice of an exponential based weighting model to allow a slow change in $w_s$ for larger values of $d_m$ at any particular $\mathrm{t_r}$. As $d_m$ gets smaller the rate of change in $w_s$ gradually increases, until rapidly reaching its upper bound infinitesimally, close to distance $d_m$ of zero. We utilize these characteristics of the exponential function to create a reduced cross-track error path following scheme, requiring less maneuvering effort for the USV group on a collision course with an erratically behaving moving obstacle.

*2) Moving obstacle path prediction and repulsive potential term weightage*

The adaptive weighting model described in Section 3.2.1 assigns a weight of $w_s$ on moving obstacle repulsion for collision avoidance in accordance with a quantified maneuvering response time $t_r$ of individual USVs in the system. This adaptive weighting model is designed to provide reduced cross-track error by allowing fast maneuvering USVs to react late and slow maneuvering USVs to react early to a detected moving obstacle based on its individual ability.

We propose path prediction and a diminishing repulsion model along the predicted path of a detected moving obstacle such that the path followed by the USV avoiding the moving obstacle:

- requires reduced maneuvering effort
- reduces cross-track error
- is safer with prediction of erratic maneuvers of the moving obstacle.

The improved system is termed as the EAW method.

Once USVs detect a moving obstacle within its FOV of radius $d$, the recorded positions of the moving obstacle are used to extrapolate its path to determine its predicted path. We denote a repulsion radius $d_{repel} < d$ within which the moving obstacle is repelled. Moving obstacle positions detected within the region of $d - d_{repel}$ around the USVs are used as the initial training data for path extrapolation. For simplicity, a cubic spline extrapolation is utilized to a path distance of $\Delta s$ with higher degree polynomial extrapolations identified to result in overfitting, determined from several trial runs. We therefore deemed the cubic order of polynomial extrapolation as sufficient given limited maneuvering ability of bodies on water. Assuming a constant velocity of the moving obstacle within the detection FOV, $Z$ equidistant points are extracted from the extrapolated path $\Delta s$, each of which hosts a repulsive potential for the USV system. The summation of the repulsive potential terms along the predicted path with $Z$ potential terms can be written as,

$$U_{repel} = w_{s1}U_1 + w_{s2}U_2 + \cdots + w_{sZ}U_Z \tag{3}$$

where $U_1, U_2, \ldots, U_Z$ are repulsive potential terms, and $w_{s1}$, $w_{s2}$ up to $w_{sZ}$ are weights for each of the $Z$ potential terms.

We define the weights $w_{s1}$, $w_{s2}$ up to $w_{sZ}$ as a diminishing series, such that $w_{s1} > w_{s2} > \cdots > w_{sZ}$ assigned to each of the predicted path points along the extrapolated $\Delta s$ path, starting from the actual position of the detected moving obstacle with repulsive term $U_1$. Assuming a decreasing geometric series (common ratio, $p < 1$) of weights, the sum of the weights must be equal to the adaptive weighting $w_s$, i.e.

$$a\left(\frac{1-p^Z}{1-p}\right) = w_s \tag{4}$$

where $a$ is the first term of the series corresponding to the weight $w_{s1}$ of the repulsive potential of the detected actual position of the moving obstacle. We solve the underdetermined system for $a$ and $p$, by choosing $a$, such that weight $a = w_{s1} = \frac{w_s}{2}$, waning with a common ratio of $p$ over the $Z$ extrapolated path points. It must be noted that $a$ must be large enough such that, the actual position of the moving obstacle is repelled strong enough to maintain a large enough safety distance.

*3) Weighted artificial potential function framework for guidance and control*

We define a set of artificial potential functions to model a leader-follower based multi-USV system interacting with its environment,

$$U_{r_i}^{r_j}(r_i, r_j) = \frac{1}{2}\eta_{11}\left(\ln\left||r_i - r_j|\right| + \frac{d_{ij}}{\left||r_i - r_j|\right|}\right) + \frac{1}{2}\eta_{12}\left(\left||r_i - r_j|\right| - d_{ij}\right)^2, \quad i, j \in I_R \tag{5}$$

$$U_{r_h}^{w_p}(r_h, w_p) = \frac{1}{2}\eta_2\left||r_h - w_p|\right|^2, \quad h \in I_R, p \in I_W \tag{6}$$

$$U_{r_i}^{m_k}(r_i, m_k) = \sum_{z=1}^{Z+1}\frac{1}{2}ap^{z-1}\eta_3\left(d_{repel} - \left||r_i - m_{k,z-1}|\right|\right)^2, \quad 0 < \left||r_i - m_{k,z-1}|\right| \le d_{repel},\ i \in I_R, k \in I_M \tag{7}$$

$$U_{r_i}^{o_l}(r_i, o_l) = \frac{1}{2}\eta_4\left(\frac{1}{||r_i - o_l||} - \frac{1}{d_{io}}\right)^2, \quad i \in I_R, l \in I_O \tag{8}$$

where $\eta_{11}$, $\eta_{12}$, $\eta_2$, $\eta_3$ and $\eta_4$ are arbitrary positive scaling constants for their corresponding potential functions.

Artificial potential function $U_{r_i}^{r_j}$ models inter-USV interaction as a function of the relative distance between pairs of USVs $R_i$ and $R_j$, with an equilibrium distance of $d_{ij}$. The leader USV $R_h$ is unaffected by the interaction of the follower USVs in the group, while the follower USVs are affected by the leader and all other USVs to form a leader-follower type swarm aggregation model.

Each optimal way point $w_i$, for $i \in I_W = \{1,2,..,P_w\}$ obtained from path planning on the top layer acts as an intermediate goal point having an attractive potential. The function $U_{r_h}^{w_p}$ models the attraction of leader $R_h$ towards the next way point location $w_p$ on the path as a function of the

relative distance between $r_h$ and $w_p$. This leads to traversing of the multi-USV system towards a final goal point cutting across intermediate way points.

We consider collision avoidance of USVs from moving obstacles in the environment as a repulsive potential. The potential function $U_{r_i}^{m_k}$ for the EAW method is derived from $U_{repel}$ in Eq. (3) with the diminishing weighting terms written as a geometric progression $ap^{z-1}, z \in \{1,2,..,Z\}$. It is the summation of the series of repulsive potential terms formed along the predicted path of a detected moving obstacle within radius $d_{repel} < d$, in contrast with the adaptively weighted (AW) method which does not consider path extrapolation; a single repulsive potential function is used with the full weighting of $w_s$. The first term in the proposed EAW method corresponds to a repulsive potential between $r_i$ and the actual position of the detected moving obstacle $m_k$ termed as $m_{k,z=0}$, with the consecutive terms formed by the $Z$ equidistant points along the predicted path of the moving obstacle denoted as $m_{k,z>0}$ within radius $d_{repel}$, dependent on the relative distance between $r_i$ and $m_{k,z}$ for dynamic obstacle avoidance. The series of the summed potential terms along the predicted path are weighted by the designed diminishing weighting series described in Section 3.2.2 such that the sum of the weights equal $w_s$ obtained from Section 3.2.1.

The function $U_{r_i}^{o_l}$ models the repulsive interaction of $R_i$ with detected static obstacles $o_l$ with influence distance $d_{io}$, as a function of the relative distance between $r_i$ and $o_l$. This ensures collision avoidance with static objects (shoreline, anchored vessels) in constrained channels of maritime environments. We assume that at initial time, $\left||r_i - r_j|\right|$, $\left||r_h - w_p|\right|$, $||r_i - m_k||$ and $\left||r_i - o_l|\right|$ are all non-zero terms.

We accommodate the applicability of our framework to various types of multi-USV teams by proposing a weighting scheme for the aforementioned set of potential functions based on USVs having different maneuverability response times. We consider a scenario where a multi-USV team following a trajectory is on a collision course with a moving object detected within $d$. For a multi-USV team capable of fast maneuvering (fast response times), collision avoidance could be prioritized much later when the object is closer; the multi-USV team may prioritize minimizing cross track error and maintaining inter-USV distances until then.

However, for a multi-USV team having slow maneuvering capabilities, collision avoidance must be prioritized sooner to allow enough time for maneuvering, over minimizing cross-track error and maintaining inter-USV distances. Thus, we model the weighted potential function of $R_i$ as,

$$U_i(r_i, r_j, r_h, w_p, m_k, o_l) = (1 - w_s)\left[\sum_{j \neq i, i \neq h} U_{r_i}^{r_j} + U_{r_h}^{w_p}\right] + \sum U_{r_i}^{m_k} + \sum U_{r_i}^{o_l} \qquad (9)$$

where $w_s \in (0,1)$ is the weighting term dependant on USV maneuvering capabilities quantified as maneuvering response time $t_r$. The resultant force on $R_i$ is therefore,

$$F_i(r_i, r_j, r_h, w_p, m_k, o_l) = (1 - w_s)\left[\sum_{j \neq i, i \neq h} \nabla U_{r_i}^{r_j} + \nabla U_{r_h}^{w_p}\right] - \sum \nabla U_{r_i}^{m_k} - \sum \nabla U_{r_i}^{o_l}. \quad (10)$$

The target orientation of $R_i$ in the next time step is set consistent with the direction of $F_i$ and the magnitude of the resultant control input $\left||F_i|\right|$ is utilized as the control $u_i$ in Eq. (1).

*3.3 Controller Analysis*

We first analyze the convergence of the USVs to inter-USV equilibrium distance $d_{ij}$ without the leader USV being affected by the followers, and no inter-USV collisions. To investigate the stability and the convergence of the multi-USV system to equilibrium inter-agent distance $d_{ij}$ using the proposed control law, we define the Lyapunov function as,

$$V(r, v) = U(r) + \frac{1}{2} v^T v \quad (11)$$

where $r \in R^{ns}$ and $v \in R^{ns}$ are stacked position and velocity vectors of $n$ robots in the system, and $U(r): R^{ns} \longrightarrow R_{>\mathbb{0}}$ is the collective potential energy of the system written as,

$$U(r) = \sum_{i=1, i \neq h}^{n} \sum_{j \neq i}^{n} U_{r_i}^{r_j}\left(\left\|r_i - r_j\right\|\right). \quad (12)$$

The collective dynamics of the multi-USV system is written as,

$$\dot{r} = v \qquad \dot{v} = -\nabla U(r) - \hat{L}(r) v \quad (13)$$

where $\hat{L}(r)$ is the Kronecker product of the fully connected multi-USV system's graph Laplacian $L(r)$ and identity matrix $I_p$.

***Proof.*** We differentiate $V(r, v)$ and substitute Eq. (13):

$$\begin{aligned} \dot{V}(r, v) &= \dot{r}^T \nabla U(r) + v^T \dot{v} \\ &= v^T \nabla U(r) + v^T\left(-\nabla U(r) - \hat{L}(r) v\right) \\ &= -v^T \hat{L}(r) v \leq 0. \end{aligned} \quad (14)$$

With $\dot{V}$ as negative semi-definite, we conclude the boundedness of $v$; we emphasize here the following two assumptions: (1) With the system being applied to a harbor setting, the multi-USV team moves slow enough (with small changes in velocity per unit time), i.e. the potential function scaling parameters are tuned relative to one another to be as small as possible; and (2) the system has a sufficiently fast refresh cycle to prevent any discontinuity in the summed potential term in Eq. (9). Therefore, we determine the uniform continuity of $\dot{V}$ by calculating $\ddot{V} = -\dot{v}^T \hat{L}(r) \dot{v} - v^T \dot{r}^T \nabla \hat{L}(r) \dot{v} - v^T \hat{L}(r) \dot{v} \leq 0$; i.e. $\dot{V} \longrightarrow 0$ as $t \longrightarrow \infty$. Therefore, following application of Barbalat's Lemma, we conclude that velocities of all follower USVs will converge, i.e., $\forall i \neq h, j: v_i = v_j$.

With the total system energy bounded $V(r,v) \leq C$, the velocities are bounded as well $\|v\| \leq \sqrt{2C}$. Bounded and matching velocities imply that inter-USV distances remain positive and constant, $\forall i \neq h, j: \|\dot{r}_i - \dot{r}_j\| = 0$. Hence,

$$\dot{U}(r) = \sum_{i=1, i\neq h}^{n} \sum_{j \neq i}^{n} (\dot{r}_i - \dot{r}_j)^T \nabla U_{r_i}^{r_j}(\|r_i - r_j\|) = 0 \tag{15}$$

implying that $U(r)$ is constant at steady state. Moreover, we also conclude $\dot{v} = -\nabla U(r)$, since $\hat{L}(r)v = 0$ due to matching velocities. With $\nabla U(r)$ as zero, the system reaches a local minimum with no change in USV velocities.

With initial conditions previously defined as $\|r_i - r_j\| \neq 0$, we also conclude that no inter-USV collision occurs in the system, since $\|r_i - r_j\| = 0$ causes $U(r) \longrightarrow \infty$ which contradicts $V(r,v) \leq C$. ■

The follower USV group's centroid is defined as,

$$\bar{r} = \frac{1}{n-1} \sum_{i=1, i\neq h}^{n-1} r_i. \tag{16}$$

The leader $R_h$ is attracted to the next way point on the path defined by the attractive artificial potential $U_{r_h}^{w_p}(r_h, w_p)$ in Eq. (6). This net movement of $R_h$ creates an asymmetry in the inter-USV interaction forces defined by the artificial potential function $U_{r_i}^{r_h}(r_i, r_h)$, resulting in the motion of the USV group.

***Lemma:*** A group of $n-1$ follower USVs and 1 leader with dynamics defined as Eq. (1), and leader-follower and follower-follower USV dynamics defined as Eq. (9), the follower USV group's centroid dynamics are governed by the leader USV's attraction and repulsion,

$$\dot{\bar{r}} = -\frac{1}{n-1} \sum_{i=1, i\neq h}^{n-1} F_{r_i}^{r_h}(\|r_i - r_h\|)(r_i - r_h) \tag{17}$$

where $F_{r_i}^{r_h}$ denotes the interaction force between $R_i$ and $R_h$.

***Proof.*** Substituting the USV dynamics and inter-USV control law from Eq. (10) in the derivative of the follower USV group centroid expression in Eq. (16),

$$\dot{\bar{r}} = \frac{1}{n-1} \sum_{i=1, i\neq h}^{n-1} \dot{r}_i \tag{18}$$

$$= -\frac{1}{n-1}\sum_{i=1,i\neq h}^{n-1}\sum_{j=1,j\neq h}^{n-1} F_{r_i}^{r_j}(\|r_i - r_j\|)(r_i - r_j) - \frac{1}{n-1}\sum_{i=1,i\neq h}^{n-1} F_{r_i}^{r_h}(\|r_i - r_h\|)(r_i - r_h).$$

Since $F_{r_i}^{r_j}(\|r_i - r_j\|) = F_{r_j}^{r_i}(\|r_j - r_i\|)$, we reorganize the summation limits to obtain,

$$\frac{1}{n-1}\sum_{i=1,i\neq h}^{n-1}\sum_{j=1,j\neq h}^{n-1} F_{r_i}^{r_j}(\|r_i - r_j\|)(r_i - r_j)$$
$$= \frac{1}{n-1}\sum_{i=1,i\neq h}^{n-2}\sum_{j=i,j\neq h}^{n-1}\left[F_{r_i}^{r_j}(\|r_i - r_j\|)(r_i - r_j) + F_{r_j}^{r_i}(\|r_j - r_i\|)(r_j - r_i)\right] = 0.$$

Therefore, the first term in Eq. (18) governing the follower-follower USV attraction and repulsion equals 0, proving that Eq. (17) holds true. ■

The adaptive weighting model defines $w_s \in (0,1)$. Thus, the inter-USV artificial potential based interaction term in Eq. (9) weighted by $1 - w_s$ never goes to zero. The USVs are also increasingly repelled by moving obstacles getting closer in the distance interval $[d, 0)$, i.e. the artificial potential based moving object repulsion term in Eq. (9) weighted by $w_s$ is never zero. The USVs are also repelled by all static obstacles within $d$. Therefore, the aforementioned proofs hold such that no inter-USV collision occurs and all USVs in the system aggregate to the defined leader USV $R_h$ in finite time. Since the leader $R_h$ is attracted to the next way point on the path, we conclude that all USVs in the group converge to consecutive way points as well.

## 4. Validation and Results

### *4.1 Validation Setup*

To validate our proposed method, we show that teams of $n$ USVs with different maneuverability response times $t_r$ can successfully navigate along its waypoints in a constrained channel with:

- reduced cross-track error and
- reduced maneuvering effort

compared to the unweighted and AW method in presence of an oncoming high-speed moving obstacle showing erratic behavior upon detection.

The Port of Los Angeles is one of the busiest and well-known ports in the United States (The Port of Los Angeles); a narrow channel within the harbor area is therefore chosen for validation of our EAW artificial potential field framework. A 1,067×1,785 pixel binary map of the LA harbor area with 1 pixel equivalent to $3.6m$ is used to generate a path along the constrained channel. The constrained A* algorithm used $72m$ as safety distance to generate the USV enclosing

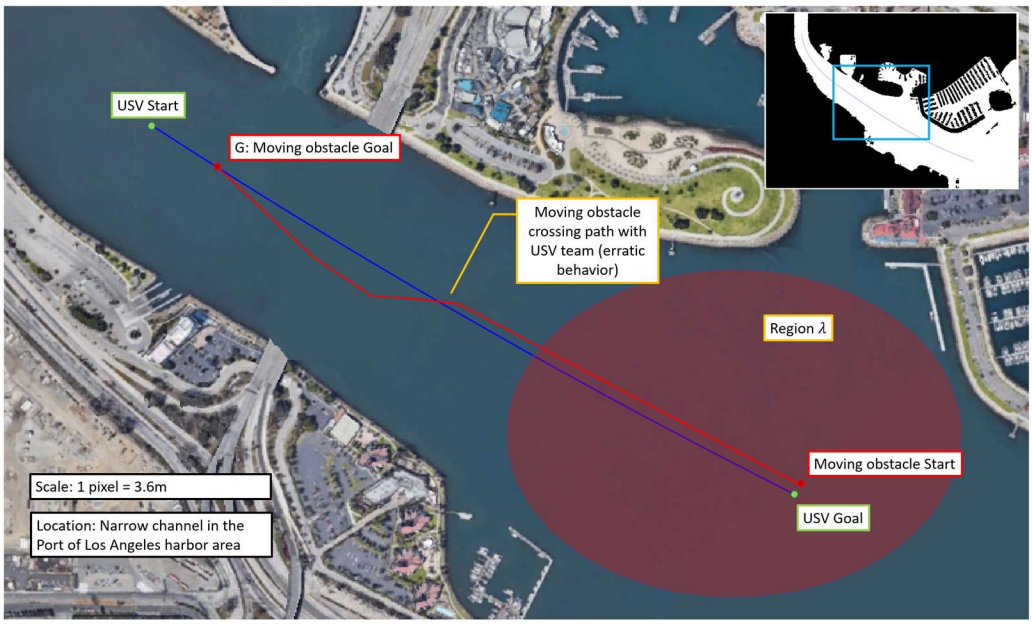


Figure 4: Experiment environment with a subset of the USV path from Layer 1 (blue) and modeled high-speed moving obstacle path (red) for dynamic obstacle avoidance validation. Area of study from the full map is shown in the subset image.

safety circle, based on the International Maritime Organization (IMO) guidelines for collision avoidance in inland water ways. The generated path is shown in Fig. 2 (right) with the identified start and the goal points. For brevity of the simulations, we use a subset of the generated waypoints over a smaller region on the map to design our validation setup. The setup is shown in Fig. 4 with the identified USV team start and goal positions (blue path). We model an oncoming high-speed moving obstacle along the generated path of the USV team such that, once within detection range the moving obstacle makes a sudden turn crossing path with the USV team (erratic behavior) followed by returning to its original heading (red path). We also define a region λ in the environment (red oval region) to be used for robustness analysis of the proposed EAW method.

We set up the validation process with a USV team of $n = 3$ having maneuverability response times of $t_r = 6$ and $t_r = 10$ in separate simulation scenarios identified as scenario 1 (S1) and scenario 2 (S2) respectively. The maneuvering response time $t_r$ depends on low-level orientation and speed controllers of each of the USVs. For validation purposes, we model maneuvering ability of individual USVs dependent on $t_r$ as $a_{max} = \frac{20}{t_r}$ and $\omega_{max} = \frac{10}{t_r}$. For each scenario, we compare the paths taken by the USV team qualitatively with time lapse images, the cross-track error of the USV team following the path and the maneuvering effort by each USV to avoid collision in terms of repulsion from the moving object and change in orientation, for the unweighted, AW and the proposed EAW artificial potential field framework. For brevity of simulations, we exaggerate the maximum allowed USV velocity to $7m/s$ and $5m/s$ in S1 and S2 respectively, and the constant velocity of the moving object approaching from the opposite direction on a collision course as $8m/s$. The moving obstacle is assumed to have a much faster maneuvering ability of $\omega_{max} = 1.4$. A collision is considered if $d_m < 10m$ and $d_{repel}$ is chosen to be $0.8d$ for all simulation cases.

*4.2 Simulation Results*

*1) Scenario S1 and S2 for a 3 USV system*

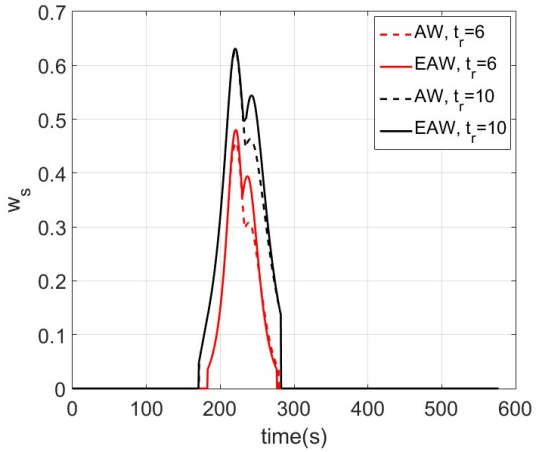


Figure 5: Observed $w_s$ in S1: $t_r = 6$ and S2: $t_r = 10$, for the $n = 3$ USV system.

Figure 6a, 6b and 6c illustrates the time lapse comparisons of the unweighted, AW and the proposed EAW methods for the S1: $t_r = 6$ simulation scenario with $n = 3$ USVs. The unweighted case time lapse shows the specific problem where the sudden change in the moving obstacles heading results in a potential failure of the framework. Upon detection of the moving obstacle slightly on the left of its path ($t = 205s$), the USVs veer to the right as a result of the repulsion from the moving obstacle; with the sudden change in heading of the moving obstacle to its left, the USVs are repelled further to their right to avoid collision and comes dangerously close to the moving obstacle ($t = 245s$) due to their limited maneuvering ability. The USV with the strongest repulsion from the moving obstacle strongly pulled the entire USV team along with it (Fig. 6e) to move further away from the path with a strong tendency to stay in formation. The actual path followed by the USV team for the unweighted case thus shows a large cross-track error as observed in Fig. 6a and Fig. 6d.

In comparison, the AW artificial potential framework allowed the USVs to react later to the moving obstacle upon detection, in accordance with its relatively fast maneuvering ability. The adaptive weighting allowed loose inter-USV interaction (Fig. 6e) and way point following when near the fast-moving obstacle so that individual USVs could avoid the moving obstacle without strongly influencing the team ($t = 230s$). The adaptive weighting also weighed moving object avoidance less until much closer to the object allowing USVs to stay on the path longer even after detection of the moving object on the path as shown in Fig. 6b ($t = 198s, 230s$). As a result, a significantly smaller cross-track error is observed in the USV path following as shown in Fig. 6d compared to the unweighted method. With the AW method, the USVs remain at a safe distance of over $50m$ from the moving obstacle, where the unweighted model brought the USVs within $15m$ and dangerously close for collision as shown in Fig. 6h.

Figure 6c visually demonstrates the effectiveness of the proposed EAW method in comparison to the already effective AW method. The moving obstacle predicted path points, repelled the USVs dependent on distance with a diminishing weight as described in Section 3.2.2

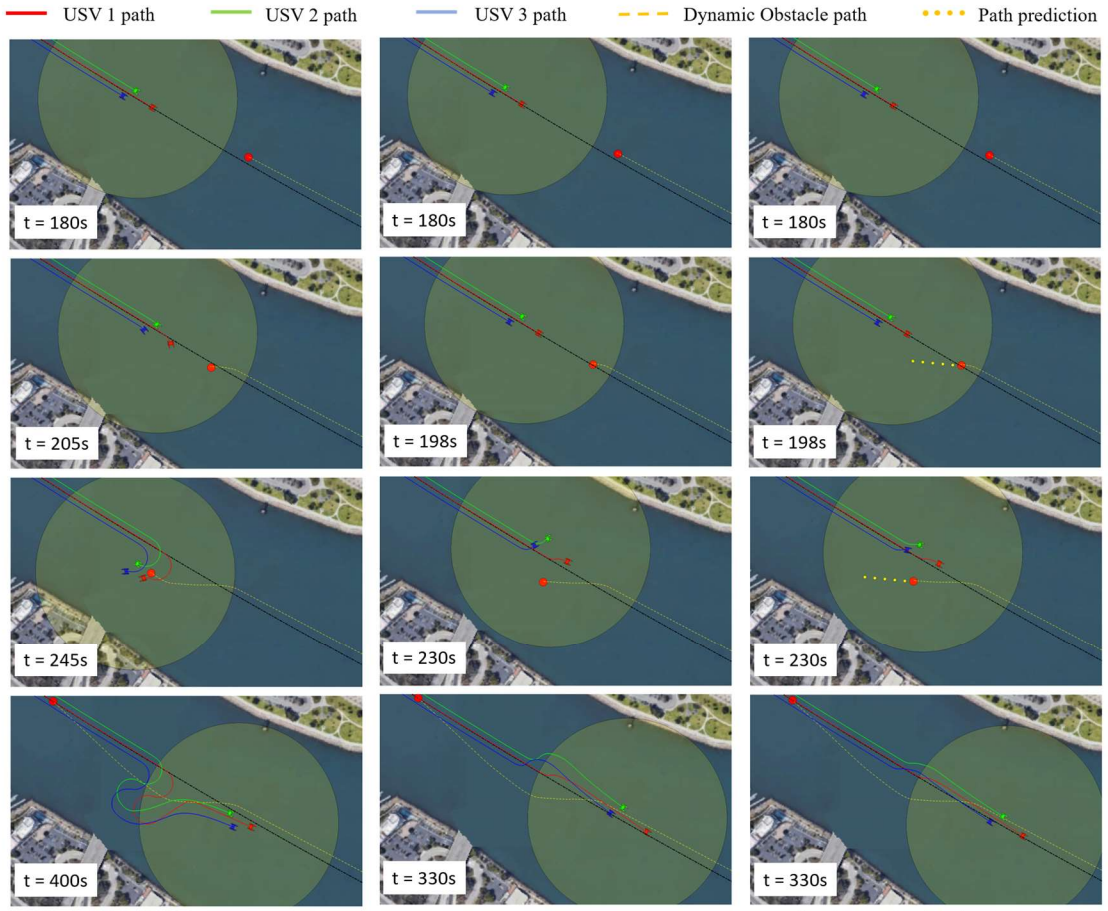


(a) Time lapse of path following and obstacle avoidance with unweighted artificial potential field.

(b) Time lapse of path following and obstacle avoidance with AW artificial potential field.

(c) Time lapse of path following and obstacle avoidance with EAW artificial potential field.

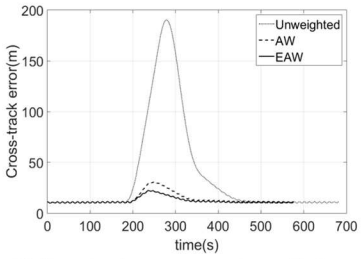


(d) Cross-track error comparison with time.

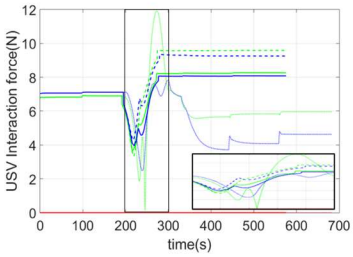


(e) Inter-USV interaction force with time.

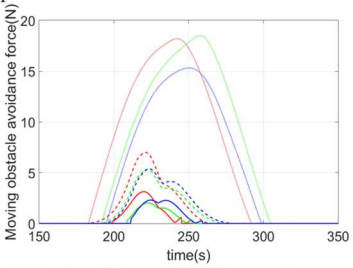


(f) Moving object and USV interaction force with time.

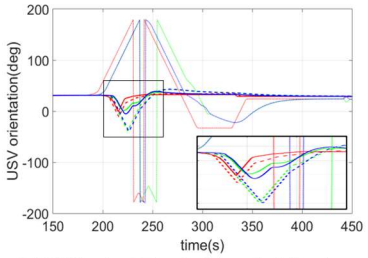


(g) USV orientation during path following with time.

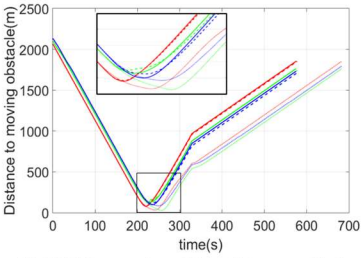


(h) USV to moving object distance with time.

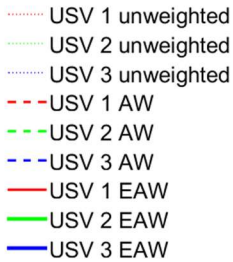


Figure 6: Simulation result for $n = 3$ USVs, on a collision course with a moving obstacle showing reduced cross-track error and maneuvering effort with the extended adaptively weighted potential framework for S1: $t_r = 6$.

from the actual moving obstacle position to the leading edge of the predicted path (Fig 6c, $t = 198s, 230s$). Thus, the USVs experienced a gradually increasing repulsive force getting closer to the moving obstacle within distance $d_{repel}$. This is observed comparing Fig. 6b, $t = 230$s and Fig. 6c, $t = 230s$; the maneuvering is less drastic for the EAW method compared to AW. This resulted in a further reduced cross-track error from the AW artificial potential field framework as observed in Fig. 6d.

The repulsive force experienced by the USVs from the moving obstacles for the 3 artificial potential field cases are shown in Fig. 6f. The unweighted artificial potential field method showed a large repulsive force over a larger duration compared to the rest as expected. The AW method showed much smaller repulsion in comparison to the unweighted and over a smaller duration. However, the proposed EAW method showed further reduced repulsive force per unit time over a much shorter duration due to the gradually increasing repulsive force experienced within distance $d_{repel}$. As a result, the maneuvering effort to avoid collision with the moving obstacle qualitatively compared as change in USV orientation in the USV orientation plot with time in Fig. 6g, showed the smallest required change in USV orientation for the proposed EAW artificial potential field framework in comparison to the rest. This suggested a much smoother actual USV path even in the presence of an erratically behaving mobile obstacle in the vicinity as observed in Fig. 6c.

The simulation with $n = 3$ USVs is repeated for the S2: $t_r = 10$ scenario. The USV group path following time lapse and resulting plots are shown in Fig. 7. With a relatively slower maneuvering response time of $t_r = 10$ the USVs were restricted by their movement capabilities and collided with the moving obstacle ($d_m < 10m$) in the unweighted artificial potential field ($t = 230s$) as seen in Fig. 7a ($t = 220s, 230s$). This is also when the repulsion force of USV 1 from the moving obstacle reaches its peak (Fig. 7f). The simulation was however allowed to proceed to observe the cross-track error which was recorded to be significantly high in comparison to the AW and EAW methods as expected (Fig. 7d).

For the AW method, the USV group having a slow maneuvering response time of $t_r = 10$ reacted relatively early to the oncoming object but gradually, proportional to the slowly increasingly weight $w_s$. The adaptive weighting plot over time is shown in Fig. 5 for both the S1 and S2 scenarios with the $n = 3$ USV system. The USVs in S2 thus experience a higher magnitude of repulsive force over a wider time duration compared to S1 as seen in Fig. 7f and 6F. This remains true for both the AW and EAW methods. This is due to the adaptive weighting model assigning a higher weight $w_s$ and over a wider elapsed time in S2 compared to S1, because of the slower maneuvering response capability of the USV in S2. The proposed EAW method was also assigned a higher weight compared to its counterpart AW method respective of its scenario S1 and S2 as expected, as with smaller cross-track error EAW allowed the USVs to remain closer to the moving obstacle. The resulting repulsive force per unit time was experienced to be less for EAW compared to AW (Fig. 7f) due to the diminishing weight model over the predicted path as described in Section 3.2.2.

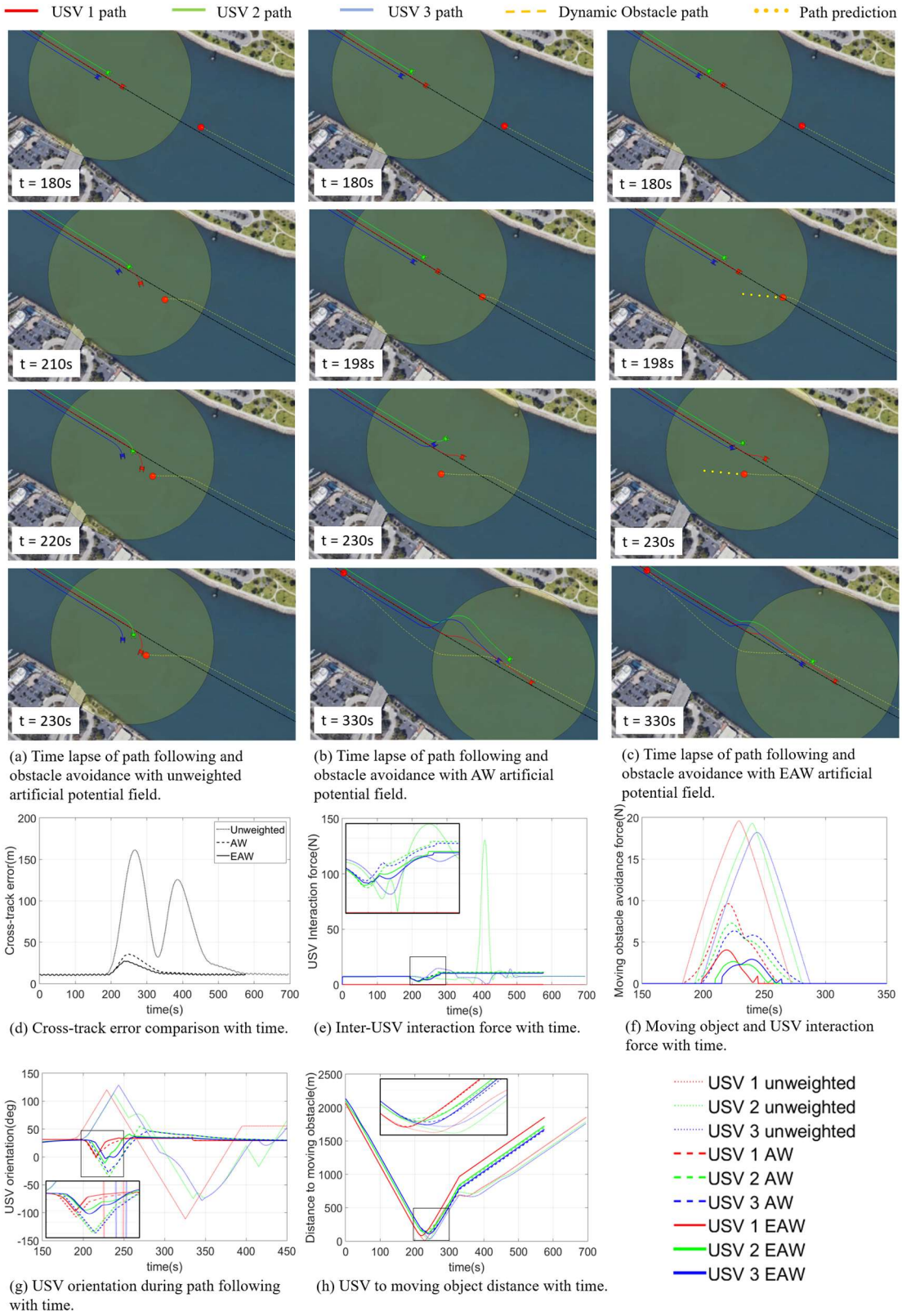


(a) Time lapse of path following and obstacle avoidance with unweighted artificial potential field.

(b) Time lapse of path following and obstacle avoidance with AW artificial potential field.

(c) Time lapse of path following and obstacle avoidance with EAW artificial potential field.

(d) Cross-track error comparison with time.

(e) Inter-USV interaction force with time.

(f) Moving object and USV interaction force with time.

(g) USV orientation during path following with time.

(h) USV to moving object distance with time.

Figure 7: Simulation result for $n = 3$ USVs, on a collision course with a moving obstacle showing reduced cross-track error and maneuvering effort with the extended adaptively weighted potential framework for S2: $t_r = 10$.

The results of S2: $t_r = 10$ for the AW and EAW methods showed similar qualitative path following results to S1: $t_r = 6$. AW allowed a cross-track error significantly less than the unweighted system while the proposed EAW method reduced it further as shown in Fig. 7d. The inter-USV forces were smaller allowing loose attraction to one another in S2 compared to S1 (Fig. Fig. 7e and 6e), due to the higher weighting $w_s$ (Fig. 5) during moving obstacle avoidance. The maneuvering repulsive force was much smaller for the EAW method compared to AW (Fig. 7f) which resulted in smaller USV orientation changes for moving obstacle avoidance (reduced maneuvering effort) with EAW as observed in Fig. 7g. This is evident by comparing Fig. 7b, $t = 230s$ and Fig. 7c, $t = 230s$ where the maneuvering is less drastic for the EAW method. Due to the slower maneuvering ability, the magnitude of USV orientation change during obstacle avoidance was recorded less for S2 compared to the S1 scenario as well (Fig. 6g and Fig 7g.) A much smoother actual USV path even in the presence of an erratically behaving mobile obstacle in the vicinity was thus observed in Fig. 7c similar to the S1 scenario.

*4.3 Discussion*

Following the validation scenarios presented, we conclude that the adaptive weighting by itself provided significant improvement in multi-USV obstacle avoidance according to USV maneuvering capabilities, while reducing cross-track error. The EAW method extended the applicability of the AW method for avoiding collisions with potentially erratically behaving moving obstacles, by utilizing detected moving obstacle path prediction and applying a diminishing repulsive potential along the predicted path based on a geometric series (common ratio, $p < 1$) dependent on distance to the detected moving obstacle.

The simulation scenarios with the maneuvering response time S1: $t_r = 6$ and S2: $t_r = 10$ were repeated for $n = 6$ robots to study the effects of larger $n$, acknowledging the fact that only a small number of USVs may be appropriate in the group at once, due to spatial and operational constraints in a narrow channel marine environment. The observations made for the $n = 6$ USV system were consistent with the $n = 3$ USV cases. Please refer to the Appendix section of this manuscript for time lapse, description and relevant plots of the 6 USV system simulations.

The simulation scenarios S1 and S2 were each repeated 20 times for $n = 3$ and $n = 6$ USVs in separate instances with varying moving obstacle trajectories in each case to analyze the robustness of the proposed EAW method. An initial start position of the moving obstacle was randomly chosen from the region $\lambda$ identified in Section 4.1 and the moving obstacle was allowed to travel along a straight line to the goal location $G$. Over the course of the 20 trials in each case, the cross-track errors remained under $40m$ with the minimum recorded as $22m$ for the proposed EAW method. Reduction in maneuvering effort for obstacle avoidance was recorded as percentage difference between the of the maximum change in USV orientation over the entire simulation duration for EAW and the unweighted method. The maximum reduction in maneuvering effort was recorded to be 83.4% while the minimum was recorded as 24.8%.

The path prediction used for the proposed EAW method relies heavily on detected moving obstacle location, which in reality suffers from uncertainty. Machine learning techniques such as Gaussian Process Machine Learning (GPML) may provide better extrapolation of the moving

obstacle path with appropriate confidence intervals. The trade-off of using such sophisticated methods is processing time and required training data for implementation. Thus, a simple cubic spline extrapolation was used in the current study considering limited maneuverability of bodies in water with a path prediction update at every iteration. Implementation of more sophisticated path prediction algorithms may be considered as an independent module following a slower update cycle than the rest of the system but must sync and be sufficiently fast enough to update the repulsive potential functions in time for dynamic obstacle avoidance. We leave detailed analysis of performance evaluation relating to update cycle on real-world experimental validation currently set as future work of our proposed method.

Any uncertainty in detected moving obstacle position is ignored with a choice of a large enough moving obstacle safety distance set as a sufficient condition. We also note relaxing the constant speed assumption of the moving obstacle within the detection radius of the USVs may provide better results; the identified equidistant $Z$ repulsion points on the plane along the predicted path could be spaced for a constant time unit in accordance with the estimated moving obstacle speed. However, for our current work we assume that the detection radius of the USVs are small enough to not provide any significant improvements over the current constant speed assumption; it would only add to the complexity of the proposed system.

In reality, autonomous multi-USV teams must also consider environmental effects such as wind, current and wakes of ships in busy harbors in the navigation control process. We assume that the proposed framework would be used as a high-level controller taking into account maneuvering ability of different types of USVs providing guidance for moving obstacle avoidance, while the USVs are equipped with low-level controllers robust enough to handle any such environmental disturbances. Therefore, for simplicity such considerations have not been made in the current validation of the proposed system.

In Layer 1, a circular safety region is considered for all USVs regardless of its shape and size, when obtaining the path using the A* algorithm. In relevance to our proposed system being directed towards USVs with different maneuvering abilities, we acknowledge that surface vehicles with an elongated shape that benefit from being able to navigate through narrow spaces is restricted in its path following capabilities following this over-simplified circular safety region implementation; an oval safety region would therefore prove to be a more appropriate assumption in such a case. Therefore, as future work we intend to incorporate better fitting safety regions for USVs of various shapes in the path planning and path following process of the proposed system.

Potential function-based systems operate relying on the overall energy state of the system. The system tends to move towards the closest minimum energy state termed as the equilibrium condition. For increasing $n$, the total energy of the system is higher and depending on the difference between the initial system potential energy state and equilibrium state, the rate at which the system tends to move towards equilibrium is also higher. Therefore, the scaling parameters for the potential functions must be tuned appropriately for significant changes in $n$. We also note that the potential function scaling parameters must be tuned to remain sufficiently small such that changes in the total potential experienced by each agent remains small. To ensure that the Lyapunov rate remains uniformly continuous, a sufficiently high system refresh rate with frequent moving obstacle prediction must be implemented. A larger detection radius from an agent ensures

larger training data for incrementally better moving obstacle path prediction. Therefore, with a longer predicted path the change in the total potential at every system update cycle contributed by the moving obstacle avoidance potential term will be smaller and gradual over a longer period until passing.

Although the proposed system with static and moving obstacle repulsion showed considerable improvement in reducing maneuvering effort for dynamic obstacle avoidance in a clear harbor setting, we acknowledge that further investigation must be made before its application in cluttered environments. Potential function-based systems often suffer from unforeseen local minima and claiming generality of application of the proposed system in any harbor setting is premature at this stage. Therefore, as future work of our multi-USV navigation framework, we intend to investigate potential local minima cases during dynamic obstacle avoidance in harbor environments and integrate possible solutions to the proposed framework along with real-world experimental validation of the system.

## 5. Conclusion

In this paper, a novel multi-USV navigation framework with path planning and extended adaptively weighted potential functions based on various maneuvering response time capabilities of various USV systems is proposed. A diminishing series of repulsive force along the predicted path of a detected moving obstacle allows. reduced cross-track error and reduced maneuvering effort for dynamic obstacle avoidance.

The system adaptively weights inter-USV interactions, USV and moving object repulsion, and leader attraction to the next way point to improve path following performance of multi-USV teams on a collision course with a moving object. The path followed to avoid dynamic obstacles offer less drastic cornering for USVs requiring less maneuvering effort using the proposed EAW method, compared to AW and the unweighted artificial potential field frameworks. Simulation results with teams of $n = 3$ and $n = 6$ USVs with one leader having fast and slow maneuvering response times at separate instances validate reduced cross-track error and reduced maneuvering effort with the proposed extended adaptively weighted framework. The significance of the proposed method in this paper is its applicability on a wide variety of USVs with different maneuvering abilities to improve dynamic obstacle avoidance and path following performance without complex dynamical model and control considerations for specific models of USVs.

## References

Abidin, Z. Z., Arshad, M., Ngah, U. & Ping, O., 2010. Control of mini autonomous surface vessel. In Proc. MTS/IEEE Oceans. pp. 1–4.

Almeida, C., Franco, T., Ferreira, H., Martins, A., Santos, R., Almeida, J. M., ... & Silva, E., 2009. Radar based collision detection developments on USV ROAZ II. In *Oceans 2009-Europe* (pp. 1-6). Ieee.

Arrichiello, F., Chiaverini, S. & Fossen, T. I., 2006. Formation control of marine surface vessels using the null-space-based behavioral control. In: Group coordination and cooperative control, pp. 1–19. Springer.

Balch, T., & Arkin, R. C., 1998. Behavior-based formation control for multirobot teams. *IEEE transactions on robotics and automation*, *14*(6), 926-939.

Bertram, V., 2008. Unmanned surface vehicles-a survey. Skibsteknisk Selskab. 1:1–14.

Beser, F., & Yildirim, T., 2018. Colregs based path planning and bearing only obstacle avoidance for autonomous unmanned surface vehicles. *Procedia computer science*, *131*, 633-640.

Bibuli, M., Singh, Y., Sharma, S., Sutton, R., Hatton, D. & Khan, A., 2018. A two layered optimal approach towards cooperative motion planning of unmanned surface vehicles in a constrained maritime environment. IFAC-PapersOnLine. 51(29):378-383.

Breivik, M. & Fossen, T.I., 2004. Path following for marine surface vessels. In: Oceans' 04 MTS/IEEE Techno-Ocean'04. 4, pp. 2282-2289. Marine Technology Society.

Caccia, M., Bibuli, M., Bono, R. & Bruzzone, G., 2008. Basic navigation, guidance and control of an unmanned surface vehicle. Autonomous Robots, 25(4):349-365.

Caccia, M., Bruzzone, G., & Bono, R., 2006. Modelling and identification of the charlie 2005 asc. In: 14th Mediterranean Conference on Control and Automation, pp. 1–6. IEEE.

Campbell, S., Abu-Tair, M. & Naeem, W., 2014. An automatic COLREGs-compliant obstacle avoidance system for an unmanned surface vehicle. Proceedings of the Institution of Mechanical Engineers, Part M: Journal of Engineering for the Maritime Environment, 228(2):108-121.

Cao, Z., Xie, L., Zhang, B., Wang, S., & Tan, M. (2003, September). Formation constrained multi-robot system in unknown environments. In *2003 IEEE International Conference on Robotics and Automation (Cat. No. 03CH37422)* (Vol. 1, pp. 735-740). IEEE.

Chao, W., Feng, M., Qing, W., & Shuwu, W., 2017. A situation awareness approach for usv based on artificial potential fields. In: 4th International Conference on Transportation Information and Safety (ICTIS), pp. 232–235. IEEE.

Chen, Y. Q. & Wang, Z., 2005. Formation control: a review and a new consideration. In: IEEE/RSJ International Conference on Intelligent Robots and Systems, pp. 3181–3186. IEEE.
Cui, R., Yang, C., Li, Y. & Sharma, S., 2017. Adaptive neural network control of AUVs with control input nonlinearities using reinforcement learning. IEEE Transactions on Systems, Man, and Cybernetics: Systems, 47(6):1019-1029.

Curcio, J., Leonard, J., & Patrikalakis, A., 2005. SCOUT-a low cost autonomous surface platform for research in cooperative autonomy. In: Proceedings of OCEANS 2005 MTS/IEEE, pp. 725-729. IEEE.

Do, K., 2012. Formation control of underactuated ships with elliptical shape approximation and limited communication ranges. Automatica, 48(7):1380–1388.

Dolan, J., Podnar, G., Stancliff, S., Low, K., Elfes, A., Higinbotham, J., Hosler, J., Moisan, T. & Moisan, J., 2009. Cooperative aquatic sensing using the telesupervised ocean sensor fleet. In Proc. Remote Sensing Ocean, Sea Ice, Large Water Regions, vol. 7473, pp. 1–12.

Dunbabin, M., & Grinham, A., 2017. Quantifying spatiotemporal greenhouse gas emissions using autonomous surface vehicles. Journal of Field Robotics, vol. 34, no. 1, pp. 151–169.

Fraga, J., Sousa, J., Cabrita, G., Coimbra, P. & Marques, L., 2014. Squirtle: An ASV for inland water environmental monitoring. In ROBOT: First Iberian Robotics Conference, pp. 33-39. Springer.

Girdhar, Y., Xu, A., Dey, B., Meghjani, M., Shkurti, F., Rekleitis, I., and Dudek, G., 2011. MARE: Marine Autonomous Robotic Explorer. In: IEEE/RSJ International Conference on Intelligent Robots and Systems (IROS), pp. 5048-5053. IEEE.

Goudey, C. A., Consi, T., Manley, J., & Graham, M. (1998). A robotic boat for autonomous fish tracking. *Marine Technology Society. Marine Technology Society Journal*, *32*(1), 47.

Guanghua, W., Deyi, L., Wenyan, G. & Peng, J., 2013. Study on formation control of multi-robot systems. In: Third International Conference on Intelligent System Design and Engineering Applications, pp. 1335–1339. IEEE.

Halterman, R., & Bruch, M., 2010. Velodyne HDL-64E lidar for unmanned surface vehicle obstacle detection. In *Unmanned Systems Technology XII* (Vol. 7692, p. 76920D). International Society for Optics and Photonics.

Huang, H., Zhu, D. & Ding, F., 2014. Dynamic task assignment and path planning for multi-auv system in variable ocean current environment. Journal of Intelligent & Robotic Systems, 74(3-4):999–1012.

Karapetyan, N., Braude, A., Moulton, J., Burstein, J.A., White, S., Kane, J., Rekleitis, I., 2019. Riverine Coverage with an Autonomous Surface Vehicle over Known Environments. In: IEEE/RSJ International Conference on Intelligent Robots and Systems (IROS), pp. 3098-3104. IEEE.

Karapetyan, N., Moulton, J., Lewis, J. S., Li, A. Q., O'Kane, J. M., & Rekleitis, I., 2018. Multi-robot dubins coverage with autonomous surface vehicles. In: IEEE International Conference on Robotics and Automation (ICRA), pp. 2373-2379. IEEE.

Kimball, P., Bailey, J., Das, S., Geyer, R., Harrison, T., Kunz, C., Manganini, K., Mankoff, K., Samuelson, K., Sayre-McCord, T., Straneo, F., Traykovski, P., and Singh, H., 2014. The WHOI

Jetyak: An autonomous surface vehicle for oceanographic research in shallow or dangerous waters. In: IEEE/OES Autonomous Underwater Vehicles (AUV), pp. 1–7. IEEE.

Jo, W., Park, J. H., Hoashi, Y., & Min, B. C., 2019. Development of an Unmanned Surface Vehicle for Harmful Algae Removal. In OCEANS 2019 MTS/IEEE SEATTLE, pp. 1-7. IEEE.

Kobilarov, M., 2012. Cross-entropy motion planning. International Journal of Robotics Research, 31(7):855–871.

Larson, J., Bruch, M. & Ebken, J., 2006. Autonomous navigation and obstacle avoidance for unmanned surface vehicles. In: Unmanned Systems Technology VIII, 6230:623007. International Society for Optics and Photonics.

Lin, X. & Liu, Y., 2018. Research on multi-usv cooperative search method. In: IEEE International Conference on Mechatronics and Automation (ICMA), pp. 2012–2018. IEEE.

Liu, Y. & Bucknall, R., 2015. Path planning algorithm for unmanned surface vehicle formations in a practical maritime environment. Ocean Engineering, 97:126-144.

Liu, Y. & Bucknall, R., 2018. A survey of formation control and motion planning of multiple unmanned vehicles. Robotica, 36(7):1019-1047.

Lu Y, Niu H, Savvaris A, Tsourdos A. Verifying collision avoidance behaviours for unmanned surface vehicles using probabilistic model checking. IFAC-PapersOnLine. 2016 Jan 1;49(23):127-32.

Mancini, A., Frontoni, E., Zingaretti, P. and Longhi, S., 2015, June. High-resolution mapping of river and estuary areas by using unmanned aerial and surface platforms. In *2015 International Conference on Unmanned Aircraft Systems (ICUAS)* (pp. 534-542). IEEE.

Manjanna, S., Li, A. Q., Smith, R. N., Rekleitis, I., & Dudek, G., 2018. Heterogeneous multi-robot system for exploration and strategic water sampling. In: 2018 IEEE International Conference on Robotics and Automation (ICRA), pp. 1-8. IEEE.

Manley, J. E., Marsh, A., Cornforth, W., & Wiseman, C., 2000. Evolution of the autonomous surface craft autocat. In: OCEANS 2000 MTS/IEEE Conference, pp. 403–408. IEEE.

Manzini, N. A. 2017. USV path planning using potential field model. Tech. Report, Naval Postgraduate School Monterey United States.

Mina, T., Singh, Y., and Min B-C., 2019. A Novel Double Layered Weighted Potential Field Framework for Multi-USV Navigation towards Dynamic Obstacle Avoidance in a Constrained Maritime Environment, In: OCEANS 2019 MTS/IEEE Conference, (pp. 1-9). IEEE.

Motwani, A., 2012. A survey of uninhabited surface vehicles. Tech. Report, Marine and Industrial Dynamic Analysis, School of Marine Science and Engineering, Plymouth University.

Moulton, J., Karapetyan, N., Bukhsbaum, S., McKinney, C., Malebary, S., Sophocleous, G., Li, A.Q. and Rekleitis, I., 2018. An autonomous surface vehicle for long term operations. In: OCEANS 2018 MTS/IEEE Charleston, pp. 1-10. IEEE.

Moulton, J., Karapetyan, N., Kalaitzakis, M., Li, A. Q., Vitzilaios, N., & Rekleitis, I., 2019. Dynamic Autonomous Surface Vehicle Controls Under Changing Environmental Forces. In: 12th Conference on Field and Service Robotics (FSR), Springer.

Naeem, W., Sutton, R. & Chudley, J., 2006. Modelling and control of an unmanned surface vehicle for environmental monitoring. In: UKACC International Control Conference, pp. 1-6.

Oh, H., Shirazi, A. R., Sun, C. & Jin, Y., 2017. Bio-inspired self-organising multi-robot pattern formation: A review. Robotics and Autonomous Systems. 91:83–100.

Peng, Z., Wang, D., Shi, Y., Wang, H. & Wang, W., 2015. Containment control of networked autonomous underwater vehicles with model uncertainty and ocean disturbances guided by multiple leaders. Information Sciences, 316:163–179.

Protei, 2011. [Online]. Available: http://sites.google.com/a/opensailing.net/protei/.

Savvaris, A., Niu, H., Oh, H. & Tsourdos, A., 2014. Development of Collision Avoidance Algorithms for the C-Enduro USV. In: Proceedings of the 19th IFAC World Congress. 47: 12174-12181.

See, H. A., 2017. Coordinated guidance strategy for multiple USVs during maritime interdiction operations. In: Master Thesis, Naval Postgraduate School Monterey, United States.

Sharma, S.K., Sutton, R., Motwani, A. & Annamalai, A., 2014. Non-linear control algorithms for an unmanned surface vehicle. Proceedings of the Institution of Mechanical Engineers, Part M: Journal of Engineering for the Maritime Environment, 228(2):146-155.

Singh, Y., Sharma, S., Sutton, R., Hatton, D. & Khan, A., 2018. A constrained A* approach towards optimal path planning for an unmanned surface vehicle in a maritime environment containing dynamic obstacles and ocean currents. Ocean Engineering, 169:187-201.

Stenersen, T., 2015. Guidance System for Autonomous Surface Vehicles. In: Master's thesis, NTNU.

The Port of Los Angeles. About the Port. Viewed on July, 2020. Available at https://www.portoflosangeles.org/about.

Thirunavukkarasu, G., Patrick, L., Champion, B., Chua, L., & Joordens, M., 2017. Design and development of a low-cost Autonomous Surface Vehicle. In *2017 12th System of Systems Engineering Conference (SoSE)* (pp. 1-6). IEEE.

Wang, N., Gao, Y., Zheng, Z., Zhao, H. and Yin, J., 2018, June. A Hybrid Path-Planning Scheme for an Unmanned Surface Vehicle. In *2018 Eighth International Conference on Information Science and Technology (ICIST)* (pp. 231-236). IEEE.

Wolf, M. T., Rahmani, A., de la Croix, J. P., Woodward, G., Vander Hook, J., Brown, D., Schaffer, S., Lim, C., Bailey, P., Tepsuporn, S. & Pomerantz, M., 2017. CARACaS multi-agent maritime autonomy for unmanned surface vehicles in the Swarm II harbor patrol demonstration. In: Unmanned Systems Technology XIX, pp. 101950. International Society for Optics and Photonics.

Xie, S., Chu, X., Zheng, M. & Liu, C., 2019. Ship predictive collision avoidance method based on an improved beetle antennae search algorithm. Ocean Engineering, 192:106542.

Xie, S., Wu, P., Peng, Y., Luo, J., Qu, D., Li, Q. & Gu, J., 2014. The obstacle avoidance planning of usv based on improved artificial potential field. In: IEEE International Conference on Information and Automation (ICIA), pp. 746–751. IEEE.

Zhao, Y., Li, W. & Shi, P., 2016. A real-time collision avoidance learning system for Unmanned Surface Vessels. Neurocomputing, 182:255-266.

**Appendix -** *Scenario S1 and S2 for a 6 USV system*

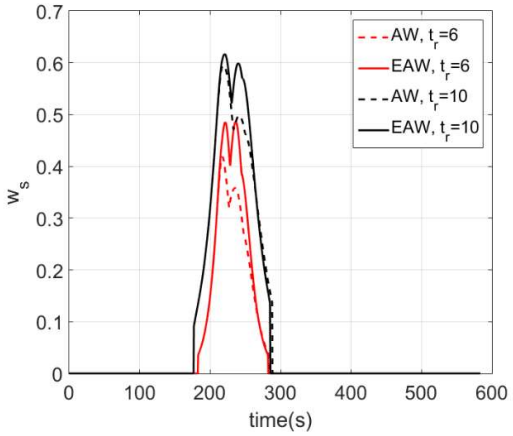


Figure A1: Observed $w_s$ in S1: $t_r = 6$ and S2: $t_r = 10$, for the $n = 6$ USV system.

We present the simulation scenarios with maneuvering response times S1: $t_r = 6$ and S2: $t_r = 10$ for $n = 6$ robots to present the effects of larger $n$, acknowledging the fact that only a small number of USVs may be appropriate in the group at once, due to spatial and operational constraints in a narrow channel marine environment. With the extended adaptively weighted potential function framework, the relatively fast maneuvering response time case (S1: $t_r = 6$) resulted in a low peak and short time spanning $w_s$ profile and the relatively slow maneuvering response time case (S2: $t_r = 10$) resulted in a higher peak spanning over a longer period of time (see Figure A1). The EAW method retained a high $w_s$ for a longer duration compared to the AW method as expected, due to the USVs remaining much closer to the moving obstacle longer, still above the set safety distance when choosing $a$ in Section 3.2.2.

For S1: $t_r = 6$, the AW method performed better in terms of obstacle avoidance compared to the unweighted method with a much efficient path in terms of distance travelled (see Figure A2). The proposed EAW method provided an even smoother followed path with a smaller corresponding cross-track error in comparison to the rest with smaller changes in USV orientation and smaller experienced repulsive force from the moving obstacle per unit time. The magnitudes of the experienced repulsive force recorded for the EAW method was consistent with the S1: $t_r = 6$ with $n = 3$ USV system case, showing loose inter-USV interactions during obstacle avoidance compared to the unweighted method.

The results for the comparatively slower maneuvering S2: $t_r = 10$ scenario for the $n = 6$ USV system remained consistent with the S2: $t_r = 10$ scenario of the previously presented $n = 3$ USV system. The limited slow maneuvering USVs collided with the oncoming high-speed moving obstacle ($d_m < 10m$) with the unweighted method. The AW method performed better than the unweighted method, consistent with the S2: $t_r = 10$ scenario of the $n = 3$ USV case in terms of smaller cross-track error, experienced moving object repulsion force and required USV change in orientation compared to the unweighted artificial potential field model. The observations of further reduced cross-track error, repulsive force per unit time resulting in smaller changes in USV orientation (maneuvering effort) remained consistent with the $n = 3$ USV simulation as well for the proposed EAW artificial potential method (see Figure A3).

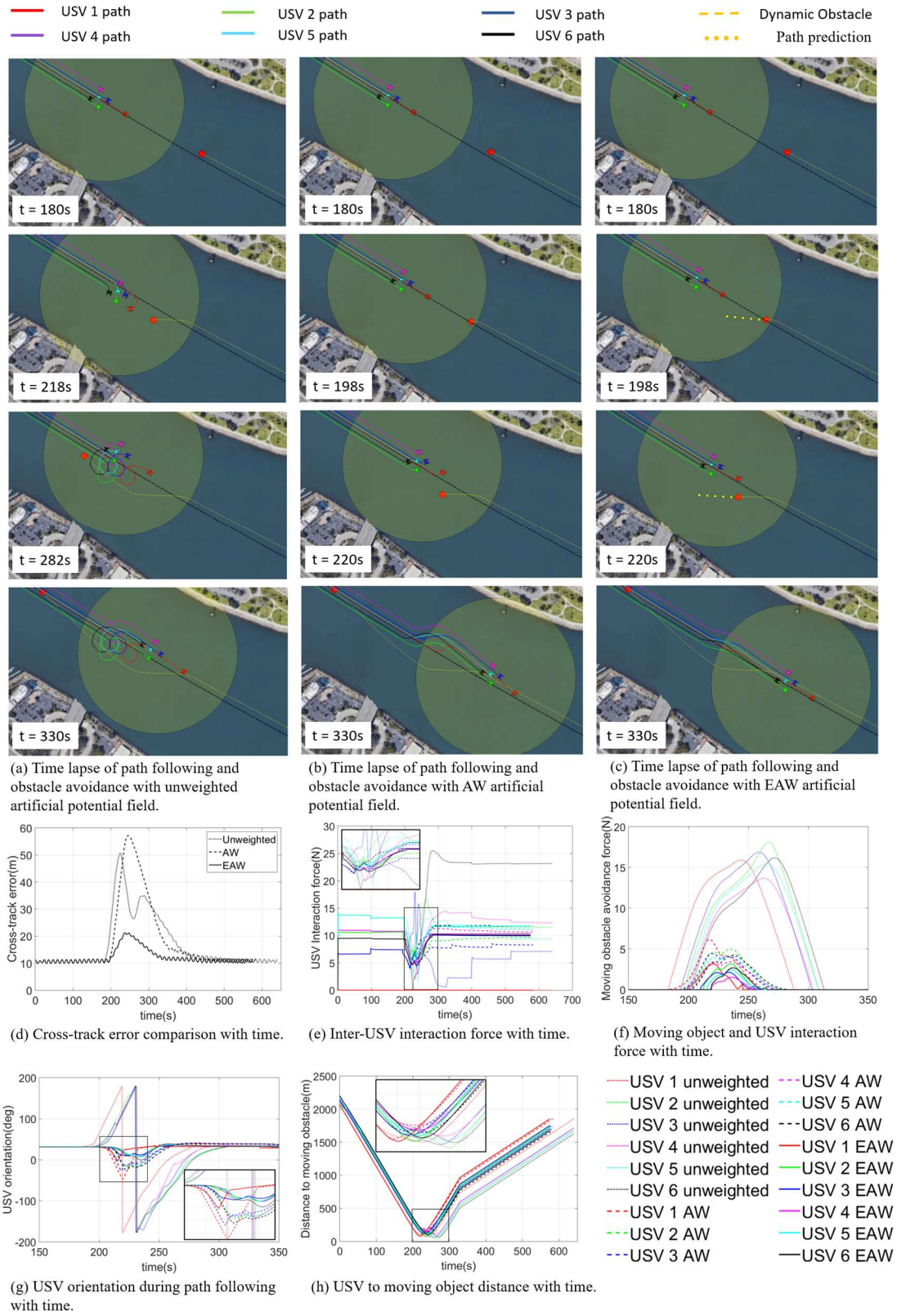


(a) Time lapse of path following and obstacle avoidance with unweighted artificial potential field.

(b) Time lapse of path following and obstacle avoidance with AW artificial potential field.

(c) Time lapse of path following and obstacle avoidance with EAW artificial potential field.

(d) Cross-track error comparison with time.

(e) Inter-USV interaction force with time.

(f) Moving object and USV interaction force with time.

(g) USV orientation during path following with time.

(h) USV to moving object distance with time.

Figure A2: Simulation result for $n = 6$ USVs, on a collision course with a moving obstacle showing reduced cross-track error and maneuvering effort with the extended adaptively weighted potential framework for S1: $t_r = 6$.

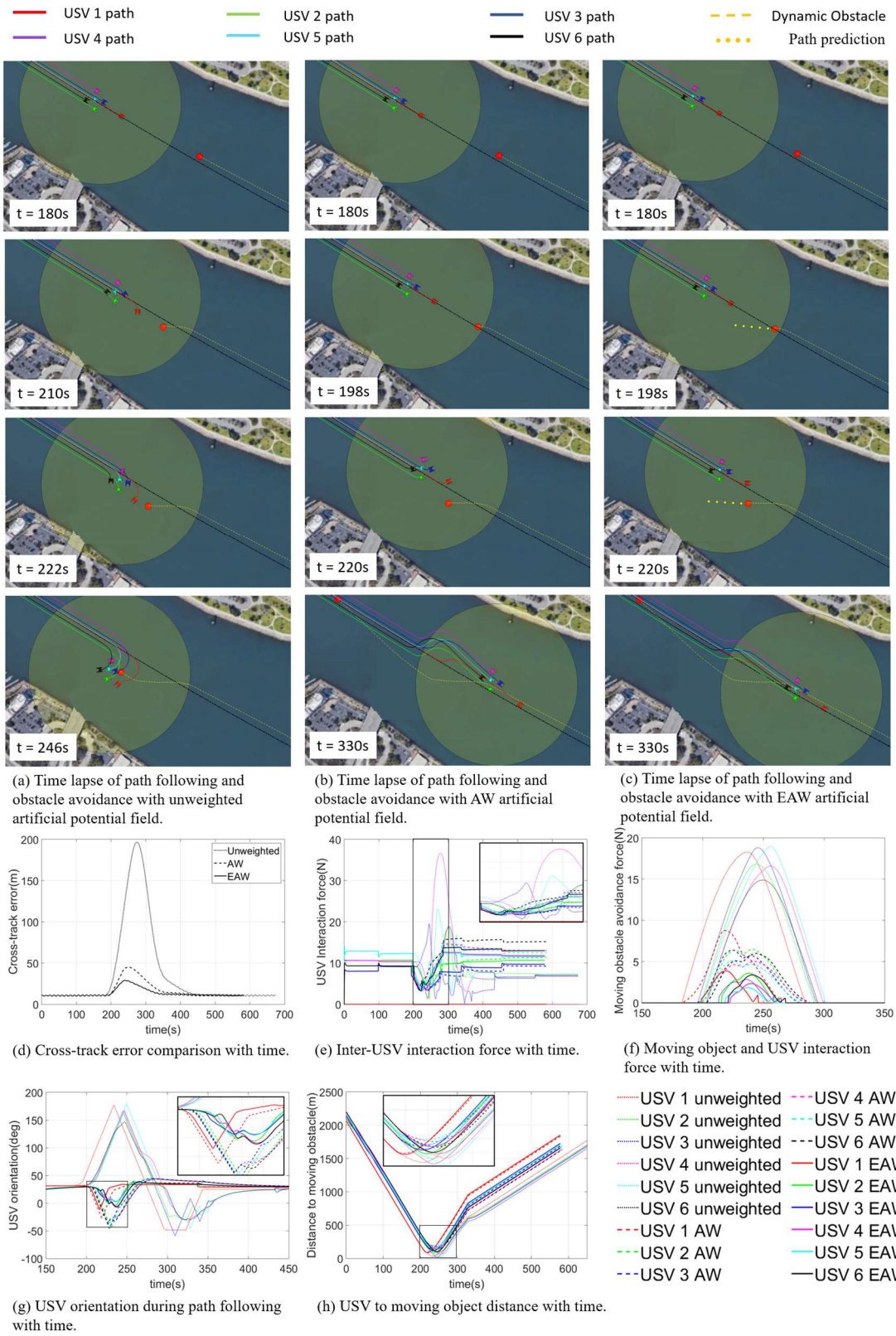


(a) Time lapse of path following and obstacle avoidance with unweighted artificial potential field.

(b) Time lapse of path following and obstacle avoidance with AW artificial potential field.

(c) Time lapse of path following and obstacle avoidance with EAW artificial potential field.

(d) Cross-track error comparison with time.

(e) Inter-USV interaction force with time.

(f) Moving object and USV interaction force with time.

(g) USV orientation during path following with time.

(h) USV to moving object distance with time.

Figure A3: Simulation result for $n = 6$ USVs, on a collision course with a moving obstacle showing reduced cross-track error and maneuvering effort with the extended adaptively weighted potential framework for S2: $t_r = 10$.

**List of figure captions:**

Figure 1: Conceptual illustration of the double layered extended adaptively weighted potential field framework for multi-USV navigation, guidance and control based on USV maneuvering capabilities to reduce cross-track error and maneuvering effort. Layer 1 generates a path from a given map and layer 2 implements path following with extended adaptively weighted collision avoidance and inter-USV dynamics.

Figure 2: Schematic of the path generated from the path planner in Layer 1 (left) in (Singh et al., 2018) and the generated path along a narrow channel in the Port of Los Angeles harbor area (right).

Figure 3: Adaptive weighting model based on moving obstacle distance $d_m$ and USV maneuvering response time $t_r$, for $K_w = 0.2$.

Figure 4: Experiment environment with a subset of the USV path from Layer 1 (blue) and modeled high-speed moving obstacle path (red) for dynamic obstacle avoidance validation. Area of study from the full map is shown in the subset image.

Figure 5: Observed $w_s$ in S1: $t_r = 6$ and S2: $t_r = 10$, for the $n = 3$ USV system.

Figure 6: Simulation result for $n = 3$ USVs, on a collision course with a moving obstacle showing reduced cross-track error and maneuvering effort with the extended adaptively weighted potential framework for S1: $t_r = 6$.

Figure 7: Simulation result for $n = 3$ USVs, on a collision course with a moving obstacle showing reduced cross-track error and maneuvering effort with the extended adaptively weighted potential framework for S2: $t_r = 10$.

Figure A1: Observed $w_s$ in S1: $t_r = 6$ and S2: $t_r = 10$, for the $n = 6$ USV system.

Figure A2: Simulation result for $n = 6$ USVs, on a collision course with a moving obstacle showing reduced cross-track error and maneuvering effort with the extended adaptively weighted potential framework for S1: $t_r = 6$.

Figure A3: Simulation result for $n = 6$ USVs, on a collision course with a moving obstacle showing reduced cross-track error and maneuvering effort with the extended adaptively weighted potential framework for S2: $t_r = 10$.